

Caspase blockade induces RIP3-mediated programmed necrosis in Toll-like receptor-activated microglia

SJ Kim¹ and Jianrong Li^{*1}

Microglia are the resident immune cells in the central nervous system and key players against pathogens and injury. However, persistent microglial activation often exacerbates pathological damage and has been implicated in many neurological diseases. Despite their pivotal physiological and pathophysiological roles, how the survival and death of activated microglia is regulated remains poorly understood. We report here that microglia activated through Toll-like receptors (TLRs) undergo RIP1/RIP3-dependent programmed necrosis (necroptosis) when exposed to the pan caspase inhibitor zVAD-fmk. Although zVAD-fmk and the caspase-8 inhibitor IETD-fmk had no effect on unstimulated primary microglia, they markedly sensitized microglia to TLR1/2,3,4,7/8 ligands or TNF treatment, triggering programmed necrosis that was completely blocked by RIP1 kinase inhibitor necrostatin-1. Interestingly, necroptosis induced by TLR ligands and zVAD was restricted to microglial cells and was not observed in astrocytes, neurons or oligodendrocytes even though they are known to express certain TLRs. Deletion of genes encoding TNF or TNFR1 failed to prevent lipopolysaccharide- and poly(I:C)-induced microglial necroptosis, unveiling a TNF-independent programmed necrosis pathway in TLR3- and TLR4-activated microglia. Microglia from mice lacking functional TRIF were fully protected against TLR3/4 activation and zVAD-fmk-induced necrosis, and genetic deletion of *rip3* also prevented microglia necroptosis. Activation of c-jun N-terminal kinase and generation of specific reactive oxygen species were downstream signaling events required for microglial cell death execution. Taken together, this study reveals a robust RIP3-dependent necroptosis signaling pathway in TLR-activated microglia upon caspase blockade and suggests that TLR signaling and programmed cell death pathways are closely linked in microglia, which could contribute to neuropathology and neuroinflammation when dysregulated.

Cell Death and Disease (2013) 4, e716; doi:10.1038/cddis.2013.238; published online 11 July 2013

Subject Category: Neuroscience

Microglia are the resident immune cells in the central nervous system (CNS) and the primary defenders that protect the CNS against pathogens and injury. However, persistent and excessive activation of microglia may result in pathological inflammation and has been shown to actively participate in many neurological disorders including acute brain injury, stroke, multiple sclerosis and neurodegenerative diseases.^{1,2} Toll-like receptors (TLRs) are a major family of pattern recognition receptors that recognize highly conserved pathogen-associated molecular patterns (PAMPs) expressed on broad microorganisms and initiate innate immune responses.³ In addition, TLRs also detect endogenous danger-associated molecular patterns, hence having key roles in infectious as well as non-infectious CNS disorders.⁴ Microglia express a repertoire of TLRs,⁵ and their engagement has been linked to neuronal⁶ and oligodendroglial damage,^{7,8} and exacerbated brain injury.⁹ As TLR-activated microglia secrete proinflammatory cytotoxic mediators, the resolution of activated microglia must be tightly regulated. It has long been recognized that the number and activity of

activated microglia in the CNS decreases as the pathogen is cleared or the insult subsides. However, the mechanisms that govern the elimination of locally activated microglia remain elusive. Activation-induced apoptosis of microglia is one mechanism that downregulates activated microglia. Nitric oxide, caspase-11, -1 and -3, and MST-1 have all been shown to mediate apoptosis of microglia activated by interferon gamma (IFN γ) or IFN γ plus lipopolysaccharide (LPS).^{10–12} Although it is evident that activated microglia can undergo caspase-dependent apoptosis, it remains to be determined whether activated microglia can adapt other cell death pathways. Dysregulation of the self-elimination process could potentially exacerbate CNS diseases, and persistently activated microglia are in fact associated with many chronic neuropathological conditions.

Necrotic cell death is traditionally viewed as a passive process caused by overwhelming stress and as a cause for inflammation due to release of intracellular materials. Accumulating evidence has now clearly demonstrated that certain type of necrotic cell death is programmed and could be

¹Department of Veterinary Integrative Biosciences, Texas A&M University, College Station, TX 77843, USA

*Corresponding author: Jianrong Li, Department of Veterinary Integrative Biosciences, Texas A&M University, Mail Stop 4458, College Station, TX 77843, USA. Tel: +1 979 862 7155; Fax: +1 979 847 8981; E-mail: jrli@cvm.tamu.edu

Keywords: necroptosis; caspase-8; RIP1; RIP3; microglia; Toll-like receptor; programmed necrosis

Abbreviations: CNS, central nervous system; HE, hydroethidine; JNK, c-jun N-terminal kinase; LPS, lipopolysaccharide; Nec-1, necrostatin-1; RHIM, receptor-interacting protein homotypic interaction motif; RIP, receptor-interacting protein; ROS, reactive oxygen species; TLR, Toll-like receptor; TNF, tumor necrosis factor α ; TNFR1, TNF receptor 1; TRIF, TIR-domain containing adapter-inducing interferon- β ; TUNEL, terminal deoxynucleotidyl transferase-mediated dUTP nick-end labeling
Received 09.5.13; revised 29.5.13; accepted 31.5.13; Edited by G Raschella

prevented. Activation of the kinase domain of receptor interacting protein 1 (RIP1) and assembly of RIP1/RIP3-containing signaling complex have been shown to trigger programmed necrosis in some cells, a process also termed necroptosis.¹³ Necrostatin-1 (Nec-1), a small tryptophan-based molecule that allosterically inhibits RIP1 kinase activity,^{14,15} prevents death receptor-induced necrosis¹⁶ and blocks oxidative oligodendroglial cell death.¹⁷ Administration of necrostatin-1 ameliorates neural injury in animal models of ischemia,^{15,18} traumatic brain injury,¹⁹ and Huntington's disease.²⁰ Although the underlying mechanism of the *in vivo* protective effect of necrostatin-1 remains to be fully established, necrostatin-1 administration in mice subjected to controlled cortical impact was associated with reduced microglial activation.¹⁹

Multiple lines of evidence have demonstrated that caspase-8, the initiator caspase of the death receptor-induced pathway of apoptosis, and its adaptor protein Fas-associated death domain (FADD) negatively regulate RIP1/RIP3-dependent programmed necrosis by cleaving and inactivating RIP1.²¹ Suppression of caspase-8 activity with the pan caspase inhibitor zVAD-fmk facilitates TNF α -induced necroptosis in cells expressing RIP3.²² Unlike TNF death receptor-induced necrosis, the details of pathogen-induced necrosis in innate immune cells have just started to emerge. Several studies have shown that when caspase-8 activity is suppressed by IETD-fmk, zVAD-fmk, or the viral caspase inhibitor CrmA, ligation of TLR3 or TLR4 results in programmed necrosis in human macrophages²³ and mouse peritoneal macrophages via RIP3.^{22,24} However, whether activated microglia, the innate immune cells in the CNS, undergo programmed necrosis remains unanswered.

In this study, we report that primary microglia activated by TLR ligations undergo apoptotic as well as necrotic cell death. Blockade of caspase-8 with zVAD-fmk or IETD-fmk markedly sensitized microglia to TNF and TLR1/2, TLR3, TLR4, and TLR7/8 ligation. Necroptosis of TLR3- and TLR4-activated microglia was further determined to be mediated by TRIF, RIP3, and downstream c-Jun N-terminal kinase (JNK) and reactive oxygen species (ROS). As necrotic cell death could elicit secondary inflammatory responses, unfolding the molecular mechanisms underlying the demise of activated microglia may hold important clues for future therapeutic intervention of CNS diseases.

Results

Distinct microglial responses to different magnitudes of TLR4 activation. LPS elicits robust immune responses in microglia via TLR4. To examine the relationship between the extent of microglial activation and microglial cell fate, we challenged primary rat microglia with increasing concentrations of LPS. Although activation of microglia with very low dose of LPS (0.1 ng/ml) promoted cell survival (Figures 1a and b) and TNF production (Figure 1d), higher concentrations of LPS (10–100 ng/ml) caused microglial cell death in a dose-dependent manner (Figures 1a–c). Production of TNF by activated microglia was dependent on the extent of microglia activation and appeared to reach the peak with 10 ng/ml LPS (Figure 1d), a concentration that also induced

significant DNA fragmentation as determined by increased number of TUNEL⁺ cells (Figure 1c). These data are in line with a previous study²⁵ and suggest that programmed cell death is an intrinsic, self-eliminating mechanism that prevents over-activation.

Next, we asked whether LPS over-activated microglia employ the classic apoptotic pathway for self-elimination. Activation of the executioner caspase-3 was evident in microglia treated with higher but not low dose of LPS (Figure 1e) and preceded apoptotic cell death (Supplementary Figure S1). As caspase-8 is an initiator caspase required for extrinsic pathways of apoptosis, we examined caspase-8 activation in live microglia after LPS stimulation with fluorescein-tagged FAM-LETD-fmk that affinity-labels activated caspase-8.²⁶ Two distinct patterns of caspase-8 activation were observed (Figure 1e): diffuse cytosolic activation (C-Casp-8) and localized subcellular activation of caspase-8 (L-Casp-8). Although L-Casp-8⁺ microglia were negative for TUNEL or activated caspase-3, many C-Casp-8⁺ microglia were also positive for TUNEL and activated caspase-3, suggesting that diffuse caspase-8 activation in cytosol leads to apoptosis (Figures 1e and f). Localized caspase-8 activation was previously also found in T lymphocytes upon antigen receptor activation and was associated with cell proliferation.²⁶ Together, these findings suggest that focally activated caspase-8 may function as a signaling molecule in complexes, while higher degree of activation in the cytoplasm initiates apoptotic cell death programme.

Microglia activated by low dose of LPS become necrotic when caspase-8 is suppressed. To examine the possible function of localized caspase-8 activation in LPS-activated microglia, we activated primary rat microglia with 0.1 ng/ml of LPS in the presence of specific caspase inhibitors. Although the pan caspase inhibitor zVAD-fmk (zVAD) had no effect on unstimulated, 'resting' microglia, it triggered rapid and massive cell death in LPS-activated microglia (Figures 2a–c). Furthermore, zVAD was similarly effective in inducing microglial cell death when added to microglia that were pre-activated with LPS and washed extensively (Supplementary Figure S2). LPS-activated microglia were also sensitive to caspase-8 inhibitor IETD-fmk (IETD) (Figures 2a and b). In contrast, caspase-3/7 inhibitor DEVD-fmk, caspase-1 inhibitor YVAD-fmk or their combination did not cause any cell death (Figures 2a and b). Microglia underwent necrotic cell death when treated with LPS/zVAD, as evidenced by increased DNA fragmentation (Figures 2d and e) and loss of plasma membrane integrity (Figures 2b–c). As *in situ* detection of fragmented DNA by TUNEL does not necessarily distinguish between apoptosis and necrosis, we then employed electron microscopic analyses. Consistent with our finding that higher magnitude of LPS/TLR4 activation induces caspase-dependent apoptosis (Figure 1e, Supplementary Figure S1), microglia activated with higher dose of LPS alone exhibited morphological characteristics of typical apoptosis, including decreased cellular volume, condensation of chromatin and intact cytoplasmic membrane (Figure 2f, middle). In contrast, zVAD greatly sensitized microglia to low level of LPS activation, leading to necrosis

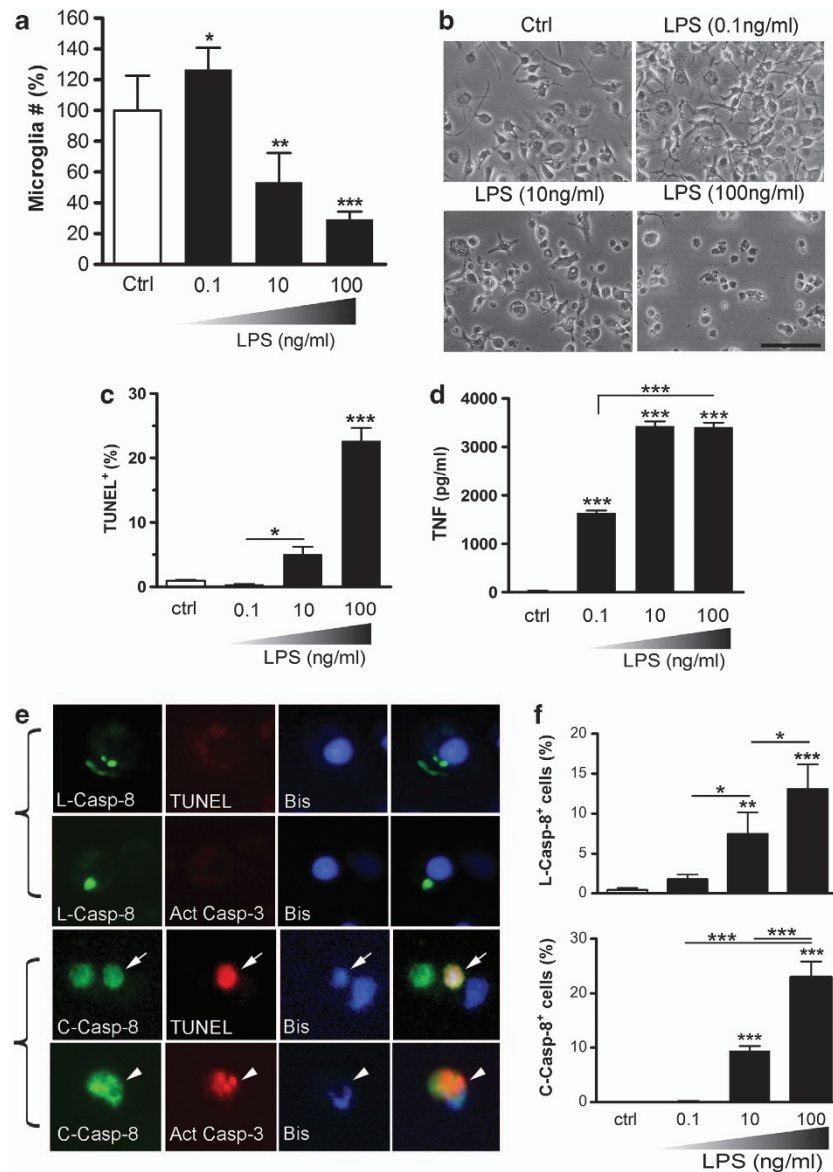


Figure 1 Microglial responses to different doses of LPS. (a) Low dose of LPS increased microglia viability whereas higher doses triggered cell death. Primary rat microglia were stimulated with increasing concentrations of LPS (0.1, 10, 100 ng/ml) for 20–24 h, and the number of microglial cells were counted. Data are a representative of three independent experiments with similar results. (b) Representative phase-contrast images of microglia treated with indicated concentrations of LPS. Scale bar, 50 μ m. (c) Significant increase of TUNEL-positive microglia after LPS stimulation for 6 h. Data represent the percentage of TUNEL-positive cells of the total cells. (d) Dose-dependent increase of TNF production upon LPS treatment for 6 h. Data are a representative of three independent experiments with similar results. (e, f) LPS-activated microglia exhibited two distinct caspase-8 activation patterns. Localized caspase-8 activation (L-Casp-8) was not associated with caspase-3 activation or cell death (upper panel, e), whereas profound cytoplasmic activation of caspase-8 (C-Casp-8) induced caspase-3 activation, DNA fragmentation (TUNEL-positive) and cell death (lower panel, e). Rat microglia were treated with 0.1–100 ng/ml LPS as above and *in situ* detection of caspase-8 activation in live cells was carried out as described in Methods section. Cells were then fixed and subjected to TUNEL labeling or immunostaining for cleaved/activated caspase-3 (act. Casp-3). Results are shown as percentage of Casp-8-positive cells of total cells. NS, not significant; * $P < 0.05$; ** $P < 0.01$; *** $P < 0.001$

that was characterized by translucent cytoplasm, organelle swelling, increased cell volume and disruption of the plasma membrane (Figure 2f). It should be mentioned that, in contrast to LPS-activated primary microglia where caspase-8 inhibitors triggered necrosis without suppressing TNF (Supplementary Figure S3), LPS/zVAD failed to cause cell death in BV-2 microglial cell line and only moderately suppressed TNF secretion (Supplementary Figure S4).²⁷ Taken together, our results demonstrate that LPS-activated

primary microglia possess at least two distinct cell death pathways depending on the extent of their activation and the presence of caspase suppressors.

Programmed necrosis induced by TLR ligands/zVAD occurs only in microglia, not in neurons, astrocytes or oligodendrocytes. As microglia express multiple TLRs, we next examined whether zVAD also causes necrosis of microglia activated by other TLR ligands such as double

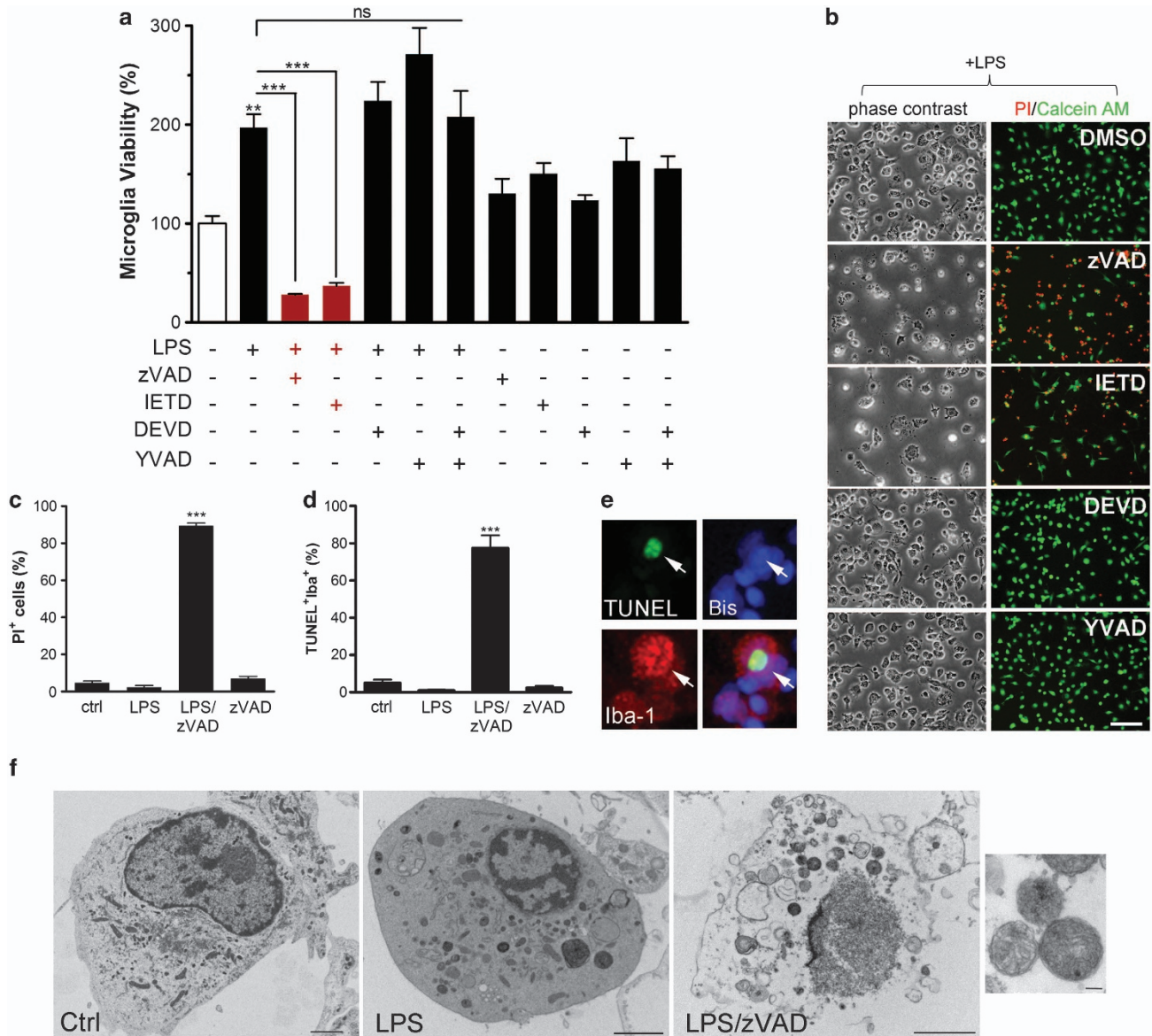


Figure 2 Microglia activated by low dose of LPS undergo rapid necrotic cell death upon caspase-8 blockade. (a–c) Inhibition of caspase-8 in LPS-activated microglia triggered a marked loss of cell viability. Primary rat microglia were stimulated with or without LPS (0.1 ng/ml) in the presence or absence of the pan caspase inhibitor, z-VAD-fmk, caspase-8 specific inhibitor IETD-fmk, caspase-3/7 inhibitor DEVD-fmk, caspase-1 inhibitor YVAD-fmk, or the combination of DEVD-fmk and YVAD-fmk (25 μ M each) for 20–24 h. Cell viability was determined by Alamar Blue assay that measures metabolic activity, and it was confirmed by live/dead cell analysis using propidium iodide (PI) and Calcein AM as described. Representative phase contrast and PI/Calcein AM staining images of microglia treated as indicated were shown. Data are representative of at least three independent experiments. Scale bar, 50 μ m. $^{**}P < 0.01$; $^{***}P < 0.001$. (d, e) LPS plus zVAD-fmk induced microglial cell death in rat mixed glial cultures that were treated with LPS (1 μ g/ml) and zVAD-fmk for 24 h. The percentage of TUNEL⁺Iba1⁺ microglia was determined. (f) Transmission electron microscopy of microglia treated with vehicle DMSO (left), 10 ng/ml of LPS alone (middle) or 0.1 ng/ml of LPS plus zVAD-fmk (10 μ M) (right) for 6 h. Microglia treated with vehicle and 10 ng/ml of LPS had intact cytoplasmic membrane, whereas many LPS/zVAD treated microglia exhibited translucent cytoplasm, swelling mitochondria (insert), and membrane breakdown. Scale bars, 2 μ m, 0.1 μ m (insert)

strained RNA mimic poly (I:C) (TLR3 ligand), Pam3CSK4 (TLR1/2), and R848 (TLR7/8). Indeed, all other TLR ligands tested induced microglial necrosis (Figure 3a). In contrast, activation of microglia with ATP (up to 1 mM) or IL-13 (100 ng/ml) plus zVAD did not cause cell death (Supplementary Figure S5), suggesting microglial necrosis specificity to death receptor and TLR activation. Interestingly, although neurons, astrocytes, and oligodendrocytes are known to express functional TNF receptor and certain TLRs, for example, TLR2/TLR3 in oligodendrocytes and

astrocytes^{28–31} and TLR3/TLR8 in neurons,^{32,33} they were not sensitive to TNF/zVAD or TLR ligand/zVAD treatment (Figures 3b–d). These results demonstrate that TNF/zVAD or TLR ligand/zVAD induces necrosis specifically in primary microglia but not in other CNS cells.

Blockade of RIP1 kinase with necrostatin-1 completely abolishes microglia necrosis. To investigate the molecular mechanism underlying TLR activation and zVAD-induced necrosis, we first tested the effect of Nec-1, which inhibits

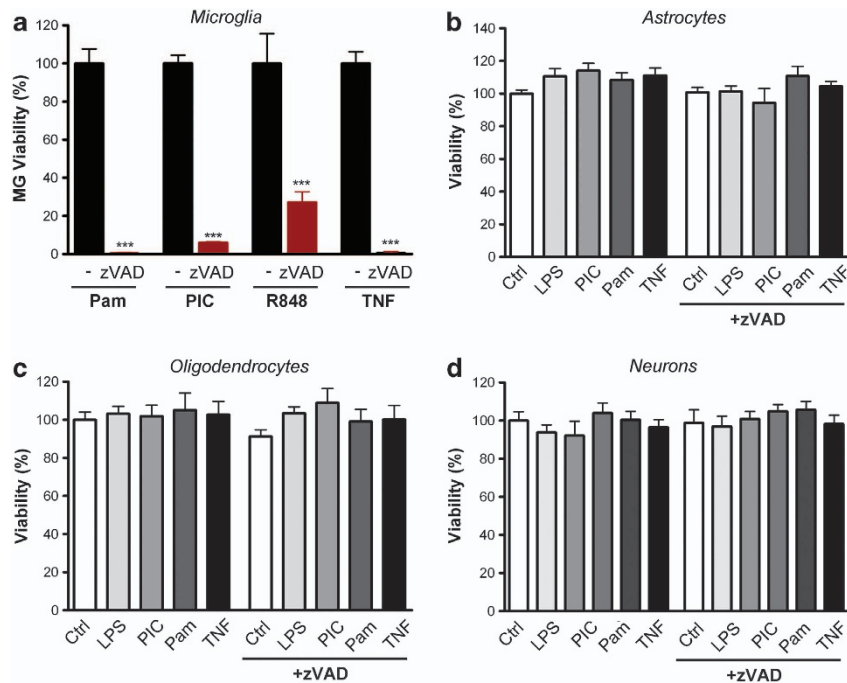


Figure 3 TLR agonists and TNF plus zVAD induce necrotic cell death only in microglia, but not in astrocytes, oligodendrocytes or neurons. (a) Primary rat microglia were treated with vehicle, TLR agonists poly(I:C) (PIC, 10 $\mu\text{g/ml}$), Pam3CSK4 (0.1 $\mu\text{g/ml}$), R848 (1 $\mu\text{g/ml}$) or TNF α (10 ng/ml) in the presence or absence of zVAD-fmk (25 μM) as indicated. Cell viability was determined 20–24 h later as described. Data represent mean \pm S.E.M. of three independent experiments. *** $P < 0.0001$. (b–d) Enriched primary astrocytes, oligodendrocytes, and neurons were treated with vehicle, LPS (20 ng/ml), poly(I:C) (50 $\mu\text{g/ml}$), Pam3CSK4 (0.5 $\mu\text{g/ml}$), R848 (5 $\mu\text{g/ml}$) or TNF α (30 ng/ml) in the presence or absence of zVAD-fmk (50 μM), and cell viability was determined 20–24 h later. No loss of cell viability was observed in astrocytes, oligodendrocytes, or neurons. Data are representative of three independent experiments

RIP1 kinase activity¹⁴ and RIP1/RIP3 association.^{34,35} Cotreatment with Nec-1 completely abolished LPS/zVAD-induced microglial cell death (Figures 4a and b). Furthermore, although RIP1 and RIP3 were endogenously expressed in unstimulated microglia, they were markedly upregulated in LPS-primed microglia at both transcription and protein levels (Figures 4c and d). This increased expression of RIP1 and RIP3 in LPS-activated microglia may account for their enhanced vulnerability to programmed necrosis. Consistently, Nec-1 was equally effective in protecting microglia against zVAD and other TLR ligand-induced cell death (Figure 4e).

TLR3 and TLR4 activation induced microglial necroptosis is independent of TNF/TNFR1 but dependent on TRIF and RIP3. Given our finding that TNF/zVAD is capable of triggering programmed necrosis in primary microglia (Figure 3a) and the fact that TNF is produced by activated microglia, we next investigated the possible involvement of autocrine TNF signaling in microglial necrosis induced by LPS/zVAD and poly(I:C)/zVAD. First, we confirmed that LPS/zVAD-induced necrosis was indeed mediated through the LPS receptor TLR4, as LPS- but not poly(I:C)-induced necroptosis was completely abrogated in *tlr4*-mutant microglia (Figure 5a). Next, we prepared mixed glial cultures from *tnf*^{+/+} and *tnf*^{-/-} mouse brains, and examined microglial survival after overnight stimulation with LPS/zVAD. Although *tnf*^{-/-} microglia were incapable of producing TNF,³⁶ they were equally susceptible as wild type to

LPS/zVAD-induced cell death (Figure 5b), suggesting that autocrine production of TNF was not necessary for LPS/zVAD-induced necrosis. In line with this, LPS/zVAD-induced loss of microglia was also independent of the TNF receptor TNFR1 (Figure 5b). Similarly, poly(I:C)/zVAD caused significant level of toxicity in both wild-type and *tnf*-deficient microglia (Supplementary Figure S6). Together, these results demonstrate the existence of alternative necrosis-initiating pathways other than the TNF/TNFR1 pathway in TLR4- and TLR3-activated microglia.

Activation of TLR3 and TLR4 is known to initiate a series of signaling cascades through various adaptors. As TRIF is a common adaptor molecule for both TLR3 and TLR4 signaling, the role of TRIF in microglial necroptosis was examined. Whereas LPS/zVAD and poly(I:C)/zVAD induced significant loss of wild-type microglia, *trif*-mutant microglia were completely protected, demonstrating a critical role for TRIF in TLR3/TLR4-activated microglial cell death (Figure 5c). To verify that TRIF indeed specifically mediated the signaling events following TLR3 ligation, TNF secretion in culture supernatants was analyzed. As expected, poly(I:C)-induced TNF production was abolished in *trif*-mutant microglia whereas LPS-induced TNF production was only transiently blocked (Figure 5d). This is consistent with the concept that TLR4 recruits adaptor molecules MyD88 and TRIF, whereas TRIF is the sole adaptor molecule for TLR3.³ One potential mechanistic link between TLR3/TLR4 activation and necroptosis is that TRIF physically interacts with RIP1 and RIP3 via receptor-interacting protein homotypic interaction motif

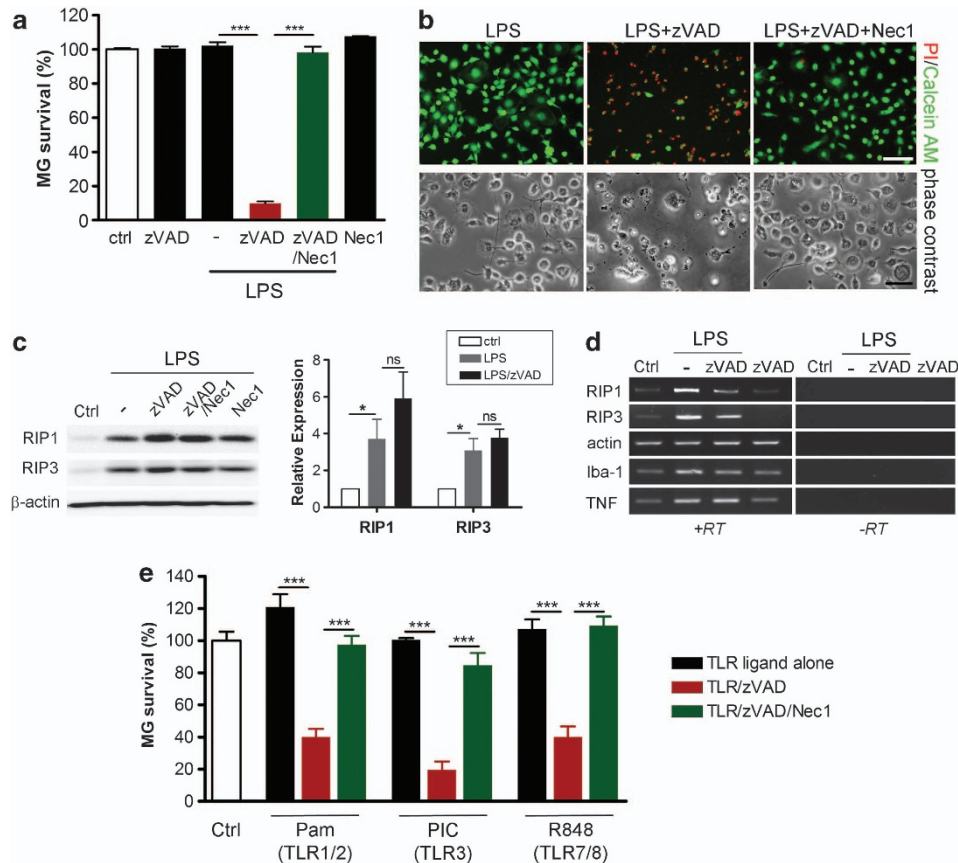


Figure 4 Blockade of RIP1 kinase activity abrogates TLR-activation-induced microglial necrosis. (a) Blockade of RIP1 kinase activity with necrostatin-1 (Nec-1) completely prevented LPS/zVAD-induced necrosis. Primary rat microglia were treated as indicated with LPS (0.1 ng/ml), zVAD (25 μ M) or Nec-1 (20 μ M), and cell survival was evaluated by cell counting. *** P <0.001. (b) Representative PI/Calcein AM (upper panel) and phase contrast (lower panel) images of microglia treated as above showing that microglial cell death induced by LPS/zVAD were abrogated by Nec-1. Data represent at least three independent experiments. Scale bars, 50 μ m. (c) LPS significantly upregulated RIP1 and RIP3 expression in microglia as determined by western blot analysis. Rat microglia were preactivated overnight with low dose of LPS, washed extensively and exposed subsequently to zVAD or zVAD/Nec-1 for 3 h. Cell lysates were then prepared and subjected to western blot analysis. A representative western blot with shorter exposure time was shown. Quantification of relative RIP1 and RIP3 expression was carried out by densitometry analyses of western blots from 3 to 7 independent experiments. * P <0.05; two-tailed student t test. (d) RT-PCR analysis of microglia treated as above, showing that LPS transcriptionally increases RIP1 and RIP3 expression. Actin and Iba1 were used as internal controls, and TNF as an indicator for microglial activation. RT, reverse transcriptase. Experiments were repeated three times with similar results. (e) Nec-1 effectively abrogated microglial necrosis induced by other TLR ligands. Microglia were treated as indicated with zVAD, Nec-1 and various TLR agonists: TLR1/2 agonist Pam3CSK4 (0.1 μ g/ml), TLR3 agonist poly(I:C) (PIC, 10 μ g/ml), or TLR7/8 agonist R848 (1 μ g/ml). Cell survival was determined by cell counting. Data represent mean \pm S.E.M. of two independent experiments. *** P <0.001

(RHIM).^{24,37} In support of this idea, *rip3* deficiency completely prevented microglia from LPS/zVAD- as well as poly(I:C)/zVAD-induced necrosis (Figure 5e), and had no effect on LPS-induced TNF production (not shown). Interestingly, *rip3*^{+/-} heterozygous microglia exhibited about 50% of the sensitivity toward LPS/zVAD or poly(I:C)/zVAD as compared with *rip3*^{+/+} microglia (Figure 5e). Therefore, in addition to RIP3 activation being a key regulatory point for necroptosis, our data also indicate that the protein expression level of RIP3 is important for effective induction of necroptosis.

Activation of JNK and production of reactive oxygen species orchestrate microglial cell demise. Previously we have shown that arachidonic acid triggers programmed necrosis in oligodendroglia through RIP1 and downstream c-jun N-terminal kinase (JNK).¹⁷ To determine whether JNK activation is required for LPS/zVAD-induced microglial necroptosis, we examined the effect of the JNK specific

inhibitor SP600125 on microglial survival. Cotreatment with SP600125 significantly but not completely prevented LPS/zVAD-induced cell death (Figure 6a), whereas blockade of p38 kinase or ERK1/2 had no protective effect (Supplementary Figure S7). Consistent with the role of JNK in microglial necrosis, robust JNK activation was observed 3 h post LPS/zVAD treatment, and was inhibited significantly by SP600125 and completely by Nec-1 (Figure 6b), indicating that JNK activation occurs downstream of RIP1.

Reactive oxygen species (ROS) production, lipid peroxidation, and lysosomal leakage have been suggested to be pivotal steps for necrosis execution in certain cell lines.¹³ As LPS-activated microglia are capable of producing reactive oxygen/nitrogen species,⁸ we reasoned that ROS scavenger butylated hydroxyanisole (BHA) may prevent LPS/zVAD-induced necrosis. Indeed, LPS/zVAD-induced microglial necrosis was almost completely mitigated by BHA (Figure 6a). In contrast and to our surprise, we did not observe

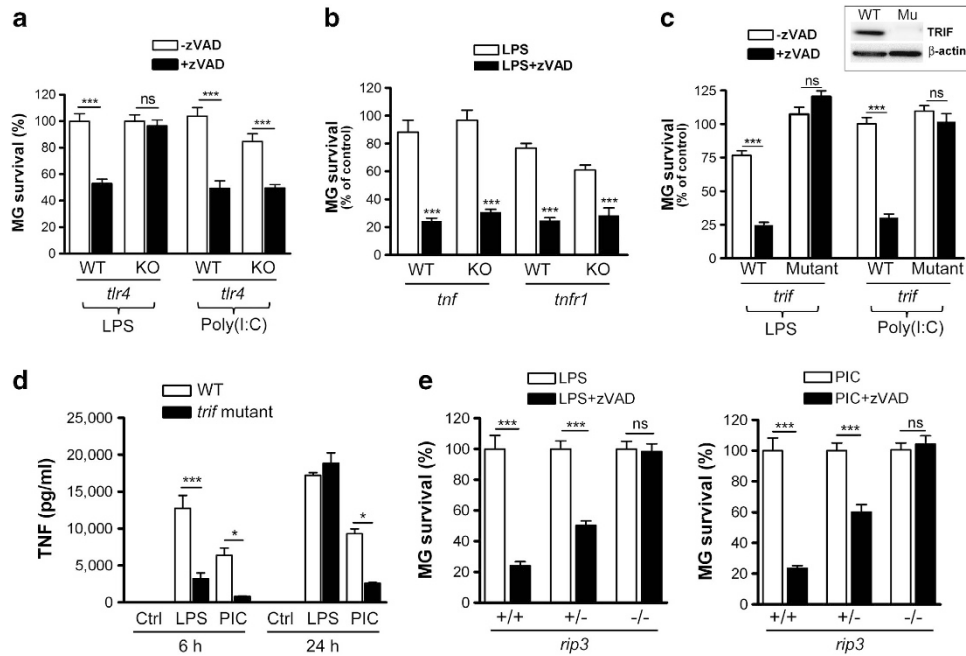


Figure 5 LPS/zVAD-induced microglial cell death is independent of TNF/TNFR1 but dependent on TRIF and RIP3. **(a)** LPS receptor TLR4 was required for LPS/zVAD-induced but not poly(I:C)/zVAD-induced microglial cell death. Mixed glial cultures from individual dissection of *tlr4* wild-type (WT) ($n = 2-5$) and knockout (KO) ($n = 3$) littermate pups were treated with vehicle, LPS ($1 \mu\text{g/ml}$), LPS/zVAD ($50 \mu\text{M}$), poly(I:C) ($50 \mu\text{g/ml}$) or poly(I:C)/zVAD for 20–24 h. Microglia survival was determined by counting Iba1⁺ cells. *** $P < 0.001$; NS, not significant. **(b)** TNF and TNFR1 were dispensable for LPS/zVAD-induced microglial necrosis. Mixed glial cultures prepared from WT and *tnf*-, *tnfr1*-deficient mice were treated with vehicle, LPS or LPS/zVAD as indicated for 20–24 h. Microglial survival was determined by counting Iba1⁺ cells. Microglia susceptibility to LPS/zVAD was the same in WT, *tnf*- and *tnfr1*-KO mixed glial cultures. Data represent three to four independent experiments. *** $P < 0.001$; NS, not significant. **(c)** TRIF was essential for LPS/zVAD- and poly(I:C)/zVAD-induced microglial necrosis. Mixed glial cultures from WT and *trif*-mutant mice were treated with LPS/zVAD or poly(I:C)/zVAD as indicated, and microglia survival was evaluated as above. Data represent mean \pm S.E.M. of at least three independent experiments. LPS/zVAD- and poly(I:C)/zVAD-induced microglial cell death was completely abrogated in *trif*-mutant cultures. *Insert*, western blot analysis of TRIF protein expression in *trif*-WT and mutant microglia. *** $P < 0.001$. **(d)** TRIF mediated poly(I:C)-induced TNF production by microglia. Mixed glia from wild-type and *trif*-mutant mice were stimulated with vehicles, LPS and poly(I:C) as specified. TNF secretion was determined by ELISA of culture supernatants from each condition at time indicated. Data represent two independent experiments with similar results. **(e)** RIP3 mediated LPS/zVAD- and poly(I:C)/zVAD-induced programmed necrosis in microglia. Mixed glial cultures derived from *rip3*^{+/+}, *rip3*^{+/-}, and *rip3*^{-/-} littermates were challenged with LPS, poly(I:C), and zVAD for 24 h, and microglial survival was determined by counting Iba1⁺ cells. Data represent mean \pm S.E.M. of three independent experiments. *** $P < 0.001$

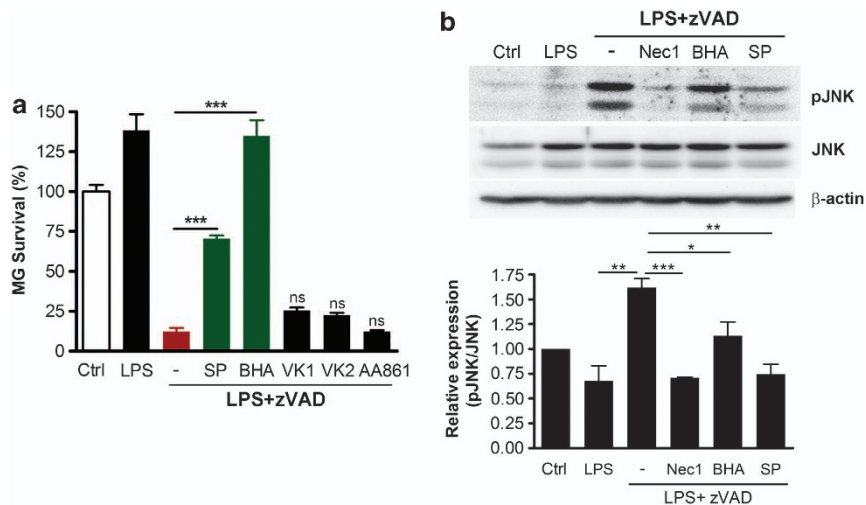


Figure 6 Reactive oxygen species (ROS) and JNK phosphorylation are required for programmed necrosis of microglia. **(a)** Abrogation of LPS/zVAD-induced microglial cell death by SP600125 ($10 \mu\text{M}$) and BHA ($150 \mu\text{M}$). Pure rat microglia were treated as indicated and cell survival was determined by counting Calcein AM⁺/PI⁻ cells 20–24 h later. Vitamin K1 ($1 \mu\text{M}$) and K2 ($1 \mu\text{M}$, Menaquinone-4) had a moderate effect but not statistically significant. AA861 ($10 \mu\text{M}$) had no protective effect. Data represent mean \pm S.E.M. of three to five independent experiments. *** $P < 0.001$; NS, not significant as compared with LPS/zVAD-treated cells. **(b)** Increased JNK phosphorylation in LPS/zVAD-treated microglia and complete inhibition by Nec-1. Rat microglia were pre-treated with vehicle, Nec-1 ($20 \mu\text{M}$), BHA ($150 \mu\text{M}$), or SP600125 ($10 \mu\text{M}$) for 1 h followed by stimulation with or without LPS (0.1 ng/ml) and zVAD ($10 \mu\text{M}$) for 3 h. Microglial lysates were then prepared and subjected to western blot analyses as described. Data represent mean \pm S.E.M. of densitometry analyses of three independent experiments. * $P < 0.05$; ** $P < 0.01$; *** $P < 0.001$; two-tailed Student's *t* test

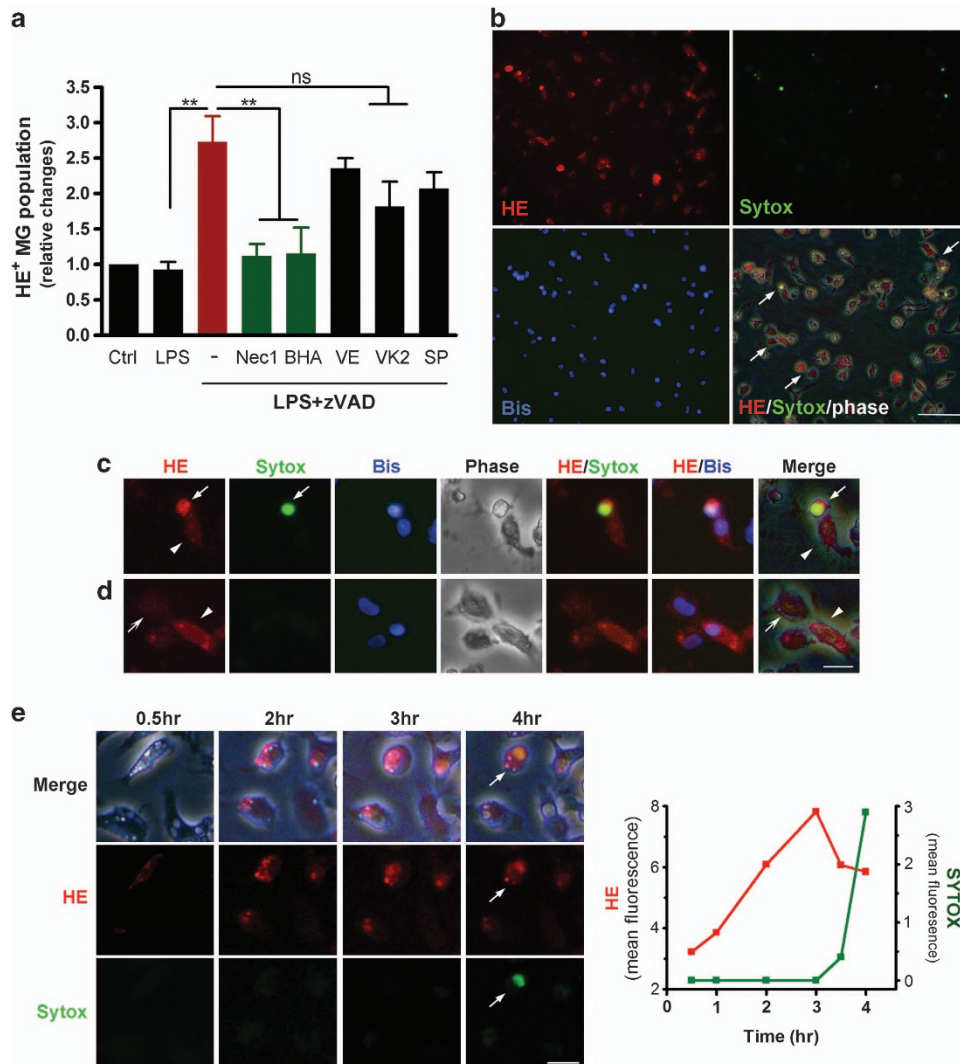


Figure 7 Elevated production of superoxide anion orchestrates microglial demise and proceeds plasma membrane permeabilization. **(a)** Increased superoxide anion production by LPS/zVAD-activated microglia and complete suppression by Nec-1 and BHA. Microglia were pre-treated with Nec-1 (20 μ M), BHA (150 μ M), vitamin E (10 μ M), vitamin K2 (10 μ M), or SP600125 (10 μ M) for 1 h prior to stimulation with low concentration of LPS (0.1 ng/ml) or LPS (0.1 ng/ml)/zVAD (25 μ M) for 3 h. Reactive oxygen species were then evaluated by the superoxide anion indicator hydroethidine (HE, 1 μ M) and flow cytometry as described. Data represent mean \pm s.e.m. of three independent experiments. ** $P < 0.01$; NS, not significant. **(b)** Representative live fluorescence and phase contrast images of microglia stimulated with LPS/zVAD for 3 h and incubated with HE (1 μ M) and Sytox (10 nM) for 20 min, showing increased oxidized HE signal preceding microglial cell death (arrows). Bisbenzimidazole was used to visualize all nuclei. Scale bar, 50 μ m. **(c, d)** Representative microglia cells in **(b)** at higher magnification, showing elevated oxidized HE signal in subpopulation of microglia (arrow in **c**, arrow head in **d**) preceding plasma membrane permeabilization in the dying cell (arrow in **c**). Stealth arrow in **(d)** indicates a microglia cell with minimum oxidized HE signal. **(e)** Time-lapse imaging analysis of microglia loaded with HE and Sytox and treated with LPS/zVAD reveals that oxidized HE signal precedes cell death. *Right*, graphic representation of the mean intensities of HE and Sytox signal of the representative cell over time. Scale bars, 15 μ m

any protection by 12-lipoxygenase inhibitor AA861, and only minor but not statistically significant protection by vitamin K1 and K2 (Figure 6a), reagents that were all highly effective in ameliorating glutathione depletion-induced oxidative injury in oligodendrocytes and neurons³⁸ as well as arachidonic acid-induced necroptosis in oligodendrocytes.³⁹ Moreover, other classic antioxidants such as hydrophilic Trolox and lipophilic vitamin E (α -tocopherol) did not confer significant protection (Supplementary Figure S8), nor did we observe significant protection by nitric oxide synthase inhibitor L-NMMA, superoxide dismutase mimic MnTMPyP, NADPH oxidase inhibitor diphenyleneiodonium, peroxynitrite decomposition catalyst

FeTMPyP or glutathione peroxidase mimic Ebselen (Supplementary Figure S7).

To further determine the role of ROS in microglial necrosis, intracellular ROS production was assessed. Unlike previous studies, we did not detect significant fluorescence signal in LPS/zVAD-treated microglia using H₂DCF-DA, a widely used general cellular oxidative stress/ROS indicator,⁴⁰ likely due to the low activation state of microglia. However, a significant increase of fluorescence signal from superoxide indicator hydroethidine (HE)⁴¹ was detected in microglia treated with LPS/zVAD for 3 h as compared with those treated with LPS alone (Figure 7a). Consistent with their effects on survival,

Nec-1 and BHA efficiently abrogated LPS/zVAD-induced HE signal whereas vitamin E and K2 did not (Figure 7a). The JNK inhibitor SP600125, although significantly and partially suppressed LPS/zVAD-induced cell death, had only limited effect on LPS/zVAD-induced increased of HE signal, suggesting that JNK activation is at the level or downstream of ROS production. This is in agreement with the observation that BHA prevented ROS production, and significantly and partially blocked LPS/zVAD-induced JNK activation (Figure 6b). Further fluorescence microscopy analyses at single cell levels revealed that LPS/zVAD-triggered superoxide production proceeded plasma membrane permeabilization and cell death (Figures 7b–e). Together, these results support the idea that excess superoxide or related species is a main source of ROS in LPS/zVAD-treated microglia. In summary, our data demonstrate that TLR4-induced microglial necroptosis is orchestrated by a series of events mediated by TRIF, RIP1/RIP3 signaling, JNK activation and specific ROS production.

Discussion

Programmed cell death is a fundamental cellular process with critical functions in development, homeostasis, and immunity. Caspase-dependent apoptosis and the recently identified programmed necrosis, also termed necroptosis, are two programmed cell death pathways that have been shown to have pivotal roles in the peripheral immune system, such as elimination of reactive T cells and innate control of viral infections.^{42–44} Microglia are the immune cells in the CNS and regulate both innate and adaptive immune responses; however, to date, to our knowledge little information is available on a necroptosis programme in microglia. In this study, we demonstrated an operation of two interconnected programmed cell death pathways in TLR-activated primary microglia: (1) caspase-dependent apoptosis in overactivated microglia, and (2) RIP3-mediated necroptosis as unmasked by caspase blockade. TLR-receptor agonists as well as TNF were capable of initiating primary microglia necrosis when caspase-8 was suppressed by zVAD-fmk or IETD-fmk, phenomena not observed in other cells of the CNS including primary neurons, astrocytes, and oligodendrocytes. The specific RIP1 kinase inhibitor, necrostatin-1, was highly effective in rescuing microglia against necroptosis. We further found that necrosis induced by ligation of microglial TLR4 or TLR3 with LPS and poly(I:C), respectively, and zVAD was independent of autocrine TNF/TNFR1 signaling and was transduced through the adaptor molecule TRIF, as LPS/zVAD and poly(I:C)/zVAD failed to cause microglial necroptosis in *trif*-mutant cells. TRIF, RIP1 and RIP3 are known RHIM motif-containing adaptor proteins capable of interacting with each other via RHIM,^{37,45} and activation of TLR3 and TLR4 in the presence of zVAD induces the formation of TRIF/RIP3 complex.²⁴ Consistent with this, genetic ablation of *rip3* completely abrogated necroptosis in microglia, demonstrating an absolute requirement for RIP3 signaling in initiating necrotic death of activated microglia. Finally, activation of JNK and generation of specific ROS appear to execute the cell death program and result in disintegration of activated microglia.

Microglia act as a first line of defense in the CNS and can be activated through TLRs in diverse situations, not only by microbial PAMPs but also by host-derived molecules liberated from damaged cells. However, the regulation of the homeostasis of activated microglia remains poorly understood. Excessive activation of microglia with LPS was associated with increased apoptotic cell death. Intriguingly, although low dose of LPS activated microglia without inducing cell death, blockade of caspase-8 triggered a robust RIP1-dependent necrosis programme. One possibility is that caspase-8 inactivates RIP1 through proteolytic cleavage,²¹ and its suppression enhances RIP1 stability, thereby sensitizing cells to RIP1-mediated necrosis. In fact, caspase-8 has been shown to possess prosurvival activities as it is required for T-lymphocyte activation,^{46,47} monocyte differentiation^{48,49} as well as suppression of TNF-induced necroptosis.^{13,21} Caspase-8 and -3/7 recently have also been implicated in microglial activation, as their blockade with IETD-fmk and DEVD-fmk suppressed LPS-induced upregulation of iNOS and certain cytokines in BV-2 microglia without triggering cell death.²⁷ We also found that caspase inhibitors did not cause BV-2 cell death and only moderately suppressed LPS-induced TNF production. In contrast, caspase blockade did not prevent LPS-induced TNF secretion in primary rat microglia, but rather markedly sensitized the cells to LPS challenge. It is noteworthy that primary rat microglia are more vulnerable than mouse microglia to TLR3/4 stimulation and caspase blockade. As caspase-8 can interact and form signaling complexes with, for example, cFLIP, FADD, RIP1/3, and TRIF under different contexts,⁵⁰ further investigation is required to delineate the exact function of caspase-8 in regulating microglial activation, survival and cell death using genetic approaches. Another interesting finding of this study is that overnight stimulation of microglia with LPS results in enhanced RIP1/RIP3 expression that predisposes the cells to necroptosis induction. The mechanism underlying LPS-induced upregulation of RIP3 remains to be defined.

ROS production has been shown to be required for necroptosis in some cell types but not others.^{35,50,51} It is interesting to note that only the lipophilic antioxidant BHA prevented TLR3/4-mediated necroptosis and was actually the antioxidant used in most of previous studies on necroptosis. Other lipophilic antioxidants, such as α -tocopherol, antioxidant enzyme mimics and lipoxygenase inhibitors, although effective in preventing arachidonic acid-induced necroptosis in oligodendrocytes,¹⁷ did not efficiently block TLR-mediated microglial necrosis. Zhang *et al.*²² also noted that only BHA prevented TNF-induced necrosis in N cells. In line with our findings, elevated levels of superoxide production in LPS/zVAD-treated microglia were found to precede cell death and was completely abolished by Nec-1 and BHA. Although we cannot exclude the possibility that BHA may have effects other than preventing superoxide production, overall our data strongly suggest that specific ROS at specific subcellular locations is required for TLR-activation-induced necroptosis in microglia.

Microglia are specified macrophages in the CNS. Recent studies have shown that microglia have a distinct embryonic origin from that of bone marrow-derived monocytes, colonize the CNS during early embryonic development, and exhibit unique features such as ramification that distinguishes them

from macrophages.⁵² However, our identification of a TLR/zVAD-induced necroptosis pathway, similar to that of macrophages,^{24,35} in microglia raises the question whether protection against necrotic microglial cell death might be beneficial in the CNS given that necrotic cell death often results in inflammation. On the other hand, it is conceivable that necroptosis is a backup strategy of innate immune cells against pathogens to stimulate the immune system when apoptosis is blocked by, for example, viruses.^{13,34} Pathological microglial cell death or degeneration has indeed been observed in mouse models of amyotrophic lateral sclerosis,⁵³ multiple sclerosis⁵⁴ and neurodegenerative diseases.⁵⁵ However, the trigger and consequences of microglial cell death remain largely unexplored and warrant further investigation.

In summary, our data revealed that microglia activated through TLRs can undergo apoptosis for self-elimination or RIP3-mediated programmed necrosis when sensitized with zVAD or under certain conditions. It thus appears that microglial TLR activation not only initiates CNS immune responses against pathogens and tissue damage, but may also be exploited to regulate the cell fate of activated microglia. Indeed, during the review process of our manuscript, a recent study reported that zVAD induces necrosis of LPS-activated microglia in mixed neuronal/glia cultures, thereby protecting neurons indirectly from LPS toxicity.⁵⁶ As microglia have critical physiological and pathological roles in many neurological disorders, detailed understanding of the mechanism that regulates the survival and death of activated microglia may provide novel strategies for targeting neurodegeneration and neuroinflammation.

Materials and Methods

Animals and reagents. Wild-type B6.129SF2/J and C57BL/6J mice, TNF α (wild-type control B6.129SF2/J, # 003008) and TNFR1 (wild-type control C57BL/6J, #003242) knockout (KO) mice, and TRIF (Ticam1, background C57BL/6J, #005037) mutant mice were obtained from the Jackson Laboratory (Bar Harbor, ME, USA). Rip3-deficient mice were generous gift from Dr. Xiaodong Wang (National Institute of Biological Sciences, China) and Dr. Astar Winoto (University of California, Berkeley). BV-2 microglial cells were kindly provided by Dr. Monica Carson (University of California, Riverside). DMEM, HBSS, propidium iodide, Calcein AM, Alamar blue, and hydroethidine were purchased from Invitrogen (Carlsbad, CA, USA). Antibody against Iba1 was from Wako chemicals (Richmond, VA, USA). Recombinant TNF, zVAD-fmk, IETD-fmk, DEVD-fmk, YVAD-fmk, and antibody against RIP1 were obtained from R&D Systems (Minneapolis, MN, USA). Rabbit anti-RIP3 and TRIF antibodies were from IMGENEX (San Diego, CA, USA). JNK, pJNK and active caspase-3 antibodies were obtained from Cell Signaling Technology (Danvers, MA, USA). Pam3CSK4 and R848 were obtained from InvivoGen (San Diego, CA, USA). JNK inhibitor II (SP600125) was from Merck (Darmstadt, Germany). MnTMPyP, OFeTMPyP, L-NMMA and Ebselen were obtained from Cayman Chemical (Ann Arbor, MI, USA). HRP-conjugated secondary antibodies were obtained from Jackson ImmunoResearch (West Grove, PA, USA). Unless specified otherwise, all other reagents were from Sigma (St. Louis, MO, USA).

Primary glial cell cultures. Primary microglia, oligodendrocytes, astrocytes, and mixed glial cultures were prepared from forebrains of 1- to 2-day-old Sprague-Dawley rat pups as described previously.^{8,36} Briefly, dissociated cells were plated onto poly-D-lysine (PDL)-coated T75 flasks or 96 well culture plates and were fed every other day with D10S (DMEM with 10% FBS) for 7–10 days. Microglia were isolated by shaking mixed glia-containing flasks for 1 h at 200 r.p.m. The purity of microglia at this stage was consistently >95%. For highly purified microglia monocultures (>99%), the cells were plated onto regular petri dishes for 1 h, detached from the plates with ice cold EBSS, and plated at final density of 3×10^4 cells per well in 96-well plates. Following 1-h pre-shaking, the flasks were shaken overnight at 200 r.p.m. to separate OL precursors (preOLs) from the

astrocyte layer. The cell suspension was then plated onto uncoated Petri dishes for 1 h to remove residual contaminating microglia, and the resulting preOLs were plated into poly-L-ornithine-coated culture plates and maintained in a serum-free basal defined medium (0.1% bovine serum albumin, 50 μ g/ml human apo-transferrin, 50 μ g/ml insulin, 30 nM sodium selenite, 10 nM D-biotin and 10 nM hydrocortisone in DMEM) supplemented with PDGF 10 ng/ml and bFGF 10 ng/ml for 5–9 days at 37 °C in a humid atmosphere of 5% CO₂ and 95% air. Astrocytes (>95%) were purified from the remaining astrocyte layer in the flask after being exposed to a specific microglia toxin L-leucine methyl ester (1 mM) for 1 h and were subcultured one to two times. Mouse mixed glial cultures were prepared with similar methods as described above from B6.129SF2/J, C57BL/6J, TRIF mutant, TNF KO, TNFR1 KO, and rip3 KO mice and were seeded in PDL-coated 96-well plates. Mixed glial cultures at DIV6-7 were used in this study.

Cell treatment and survival determination. Microglia monocultures were washed two times with D1S (DMEM containing 1% FBS) and treated in triplicate with vehicle, LPS, Pam3CSK4, R848, poly(I:C), or TNF α in the presence or absence of zVAD-fmk or IETD-fmk as specified. For mixed glial cultures, cells were treated in serum-free basal defined medium.³⁰ As microglia in mixed glial cultures were not as sensitive as in isolated pure cultures to LPS/zVAD-induced necroptosis, higher concentrations of LPS and poly(I:C) were used. Microglial survival was determined by counting Iba1⁺ cells with normal nuclei in mixed glia cultures or Calcein AM⁺/propidium iodide (PI)⁻ cells in pure microglia cultures. Total number of cells was revealed by staining all nuclei with Hoechst 33342. Five to ten random consecutive fields were counted in each well under 100 \times or 200 \times magnification, with a total of >1000 cells counted in the control condition. In some cases, cell viability in monocultures was determined by measuring cell metabolic activity using Alamar Blue, a tetrazolium dye that is reduced by living cells to a colored product as previously described.^{38,57}

For experiments involving RNA and protein isolation, primary microglia were seeded into six-well plates at a density of $1.5\text{--}2 \times 10^6$ cells/well in D10S. After attachment, the cells were washed twice with D1S, and pre-treated with LPS (0.1 ng/ml) for 12–16 h. At the end of LPS treatment, microglia were washed twice with D1S and incubated with Nec-1, butylated hydroxyanisole (BHA), SP600125, or corresponding vehicle for 1 h before the induction of necrosis with zVAD-fmk addition. Microglia were then collected with ice-cold PBS at 1 h (RNA extraction) and 3 h (protein preparation) post zVAD-fmk treatment. Vehicles used were PBS for LPS, DMSO for zVAD-fmk, Nec-1, and SP600125, and ethanol for BHA, and these were used at the same final concentration volume (<0.1%) as the corresponding reagent.

In situ caspase-8 activity assay. To detect caspase-8 activity *in situ* in living microglia, a caspase-8 detection kit containing a specific and fluorescent FAM-LETD-fmk that covalently labels active caspase-8 was used according to the manufacturer's instruction (Image-iTs LIVE Green Caspase-8 Detection Kit, Invitrogen, Carlsbad, CA, USA). After live labeling of active caspase-8, microglia were fixed and subjected to immunocytochemistry as specified in the Figure 1 legend. Images were captured using a fluorescence microscope equipped with an Olympus DP70 digital camera. On the basis of the intracellular location of active caspase-8, the percentage of microglia with cytoplasmic diffuse caspase-8 signal (C-casp-8) and localized active caspase-8 (L-casp-8) was counted and analyzed across treatment conditions.

Detection of intracellular ROS. Intracellular ROS production was evaluated by flow cytometry using the superoxide indicator hydroethidine (HE)^{41,58,59} and visualized by fluorescence microscopy. Briefly, freshly isolated primary rat microglia were treated in suspension as specified in Figure 7 legend. At the end of the treatment, cells were incubated with 1 μ M HE and 10 nM Sytox green nucleic acid stain for 20 min at 37 °C, centrifuged at 100 \times g, resuspended in 100 μ l of PBS containing 2% FBS and analyzed immediately using a flow cytometer equipped with 488 nm laser for excitation (Accuri C6, BD Biosciences, San Diego, CA, USA). Data were collected using FL1 for Sytox green nucleic acid stain (530 \pm 15 nm) or FL2 channel for HE (585 \pm 20 nm). A minimum of 10 000 cells were analyzed per condition. For time lapse microscopy, microglia seeded in slide chambers were loaded with 1 μ M HE and 10 nM Sytox for 20 min, washed and subjected to LPS (0.1 ng/ml)/zVAD-fmk (25 μ M) stimulation. Images were manually acquired from the same chamber field at specified time points. To minimize photobleaching, cells were imaged with <0.5 s of exposure time for each filter. Fluorescence intensity of representative cells was analyzed with Image J (National Institutes of Health, Bethesda, MD, USA).

Reverse transcription -PCR. Transcriptional expression levels of RIP1, RIP3, Iba1, TNF α , and β -actin in microglia upon stimulation with LPS and zVAD-fmk were examined as described previously.⁵⁷ Using Tri reagent, total RNA was extracted according to the manufacturer's instructions. Residual DNA was digested by incubating RNA samples with DNase I for 15 min at room temperature followed by DNase inactivation at 65 °C for 10 min according to the manufacturer's instructions (Invitrogen). The samples were reverse transcribed to cDNA using the reverse transcription system kit (Promega, Madison, WI, USA) as described previously.⁵⁷ Primers specific for β -actin were used as a loading control. All products were amplified by PCR using 50 ng of cDNA and the following specific primers: RIP1, forward 5'-GCACCAGCTGTCAGGGCCAG-3', reverse 5'-GCCAGCTTTCGGGACAGT-3'; RIP3, forward 5'-ACCTTGGCTGGCACTC CCA-3', reverse 5'-CCCCTGCCGAAGTGTGCTGG-3'; TNF α , forward 5'-GCC CAGCTCGTAGCAAC-3', reverse 5'-GCAGCCTTGTCCCTGAA-3'; Iba1, forward 5'-CTTTTGGACTGCTGAAAGCC-3', reverse 5'-GTTTCTCCAGCATC GCTTC-3'; and β -actin, forward 5'-AGACTTCGAGCAGGAGATGG-3', reverse 5'-CCATCATGAAGTGTGACGTTG-3'. After the PCR reaction, products were electrophoresed on 2% agarose gels and visualized under UV light using a Bio-Rad Chemidoc XRS gel documentation system and Quantity-one software.

TNF α ELISA. TNF α levels in culture supernatants were determined using a commercially available ELISA kit according to the manufacturer's instruction (eBioScience). Absorption at 450 nm was determined with a microplate reader (Fluostar Optima, BMG Labtech, Cary, NC, USA). The detection limits of the TNF ELISA were 8 pg/ml for mouse TNF α and 16 pg/ml for rat TNF α .

Transmission electron microscopy. After a quick wash with PBS, microglia were fixed in 1% glutaraldehyde and 4% paraformaldehyde (Electron Microscopy 225 Sciences, Hatfield, PA, USA) in 0.1 M, pH 7.4 phosphate buffer overnight at 4 °C. Following three washes with 8% sucrose in 0.1 M phosphate buffer, the cells were washed again in 0.1 M sodium cacodylate buffer and stained with 1% osmium tetroxide and 0.5% potassium ferrocyanide in 0.5% sucrose for 1.5 h. The cells were then dehydrated in ascending alcohol series and embedded in epoxy resin. Ultrathin sections of microglia were examined using an FEI Morgagni 268 transmission electron microscope at an accelerating voltage of 80 kV. Digital images were acquired with a MegaViewIII camera operated with iTEM software (Olympus Soft Imaging Systems, Germany).

Immunostaining, TUNEL and immunofluorescence microscopy. After the treatment, microglia were fixed with 4% paraformaldehyde at room temperature for 10 min. Cells were rinsed three times with TBS, and blocked with TBS-T (0.1% Triton X-100) containing 5% goat serum for 1 h at room temperature. Primary antibody against Iba1 (1:2000) was used for detecting microglia. Antibody against cleaved, active caspase-3 (1:1000) was used to evaluate caspase-3 activation. After overnight incubation at 4 °C, secondary antibodies conjugated with Alexa Fluor 488 or Alexa Fluor 594 (1:1000; Invitrogen) were used. Nuclei were stained with Hoechst 33342. To label fragmented DNA, TUNEL was performed using an *in situ* cell death detection kit (Roche, Indianapolis, IN, USA). All images were captured with an inverted fluorescence microscope equipped with an Olympus DP70 digital camera (model IX71; Olympus, Tokyo, Japan).

Statistical analysis. All cell culture treatments were performed in at least triplicate samples. GraphPad prism software (San Diego, CA, USA) was used for data analyses. Data were expressed as mean \pm S.E.M. and analyzed by one-way ANOVA followed by Bonferroni's *post hoc* test unless stated otherwise. Differences were considered to be statistically significant when $P < 0.05$.

Conflict of Interest

The authors declare no conflict of interest.

Acknowledgements. We are grateful to Dr. Xiaodong Wang and Dr. Astar Winoto for providing the RIP3-deficient mice; Dr. Monica Carson for the BV-2 cells, and Dr. Beiyan Zhou for allowing us to use her flow cytometer. We thank Dr. Ross Payne for his excellent technical support in TEM and Li lab members for technical assistance and discussions. This study was funded by research grants NS060017

from the National Institutes of Health and RG3975 from the National Multiple Sclerosis Society.

1. Hanisch U-K, Kettenmann H. Microglia: active sensor and versatile effector cells in the normal and pathologic brain. *Nat Neurosci* 2007; **10**: 1387–1394.
2. Block ML, Zecca L, Hong JS. Microglia-mediated neurotoxicity: uncovering the molecular mechanisms. *Nat Rev Neurosci* 2007; **8**: 57–69.
3. Kawai T, Akira S. The role of pattern-recognition receptors in innate immunity: update on Toll-like receptors. *Nat Immunol* 2010; **11**: 373–384.
4. Hanke ML, Kielian T. Toll-like receptors in health and disease in the brain: mechanisms and therapeutic potential. *Clin Sci (Lond)* 2011; **121**: 367–387.
5. Olson JK, Miller SD. Microglia initiate central nervous system innate and adaptive immune responses through multiple TLRs. *J Immunol* 2004; **173**: 3916–3924.
6. Lehnardt S. Innate immunity and neuroinflammation in the CNS: the role of microglia in Toll-like receptor-mediated neuronal injury. *Glia* 2010; **58**: 253–263.
7. Lehnardt S, Lachance C, Patrizi S, Lefebvre S, Follett PL, Jensen FE *et al*. The toll-like receptor TLR4 is necessary for lipopolysaccharide-induced oligodendrocyte injury in the CNS. *J Neurosci* 2002; **22**: 2478–2486.
8. Li J, Baud O, Vartanian T, Volpe JJ, Rosenberg PA. Peroxynitrite generated by inducible nitric oxide synthase and NADPH oxidase mediates microglial toxicity to oligodendrocytes. *Proc Natl Acad Sci USA* 2005; **102**: 9936–9941.
9. Wang Y-C, Lin S, Yang Q-W. Toll-like receptors in cerebral ischemic inflammatory injury. *J Neuroinflammation* 2011; **8**: 134.
10. Lee J, Hur J, Lee P, Kim JY, Cho N, Kim SY *et al*. Dual role of inflammatory stimuli in activation-induced cell death of mouse microglial cells. *J Biol Chem* 2001; **276**: 32956–32965.
11. Yun HJ, Yoon J-H, Lee JK, Noh K-T, Yoon K-W, Oh SP *et al*. Daxx mediates activation-induced cell death in microglia by triggering MST1 signalling. *Embo J* 2011; **30**: 2465–2476.
12. Takeuchi H, Wang J, Kawanokuchi J, Mitsuura N, Mizuno T, Suzumura A. Interferon- γ induces microglial-activation-induced cell death: A hypothetical mechanism of relapse and remission in multiple sclerosis. *Neurobiol Dis* 2006; **22**: 33–39.
13. Vanlangenakker N, Vanden Berghe T, Vandenabeele P. Many stimuli pull the necrotic trigger, an overview. *Cell Death Differ* 2012; **19**: 75–86.
14. Degtrev A, Hitomi J, Gernscheid M, Chen IL, Korkina O, Teng X *et al*. Identification of RIP1 kinase as a specific cellular target of necrostatins. *Nat Chem Biol* 2008; **4**: 313–321.
15. Degtrev A, Huang Z, Boyce M, Li Y, Jagtap P, Mizushima N *et al*. Chemical inhibitor of nonapoptotic cell death with therapeutic potential for ischemic brain injury. *Nat Chem Biol* 2005; **1**: 112–119.
16. Vandenabeele P, Galluzzi L, Vanden Berghe T, Kroemer G. Molecular mechanisms of necroptosis: an ordered cellular explosion. *Nat Rev Mol Cell Biol* 2010; **11**: 700–714.
17. Kim S, Dayani L, Rosenberg PA, Li J. RIP1 kinase mediates arachidonic acid-induced oxidative death of oligodendrocyte precursors. *Int J Physiol Pathophysiol Pharmacol* 2010; **2**: 137–147.
18. Northington FJ, Chavez-Valdez R, Graham EM, Razdan S, Gauda EB, Martin LJ. Necrostatin decreases oxidative damage, inflammation, and injury after neonatal HI. *J Cereb Blood Flow Metab* 2011; **31**: 178–189.
19. You Z, Savitz SI, Yang J, Degtrev A, Yuan J, Cuny GD *et al*. Necrostatin-1 reduces histopathology and improves functional outcome after controlled cortical impact in mice. *J Cereb Blood Flow Metab* 2008; **28**: 1564–1573.
20. Zhu S, Zhang Y, Bai G, Li H. Necrostatin-1 ameliorates symptoms in R6/2 transgenic mouse model of Huntington's disease. *Cell Death and Dis* 2011; **2**: e115.
21. Green D, Oberst A, Dillon C, Weinlich R, Salvesen G. RIPK-dependent necrosis and its regulation by caspases: a mystery in five acts. *Molecular Cell* 2011; **44**: 9–16.
22. Zhang D-W, Shao J, Lin J, Zhang N, Lu B-J, Lin S-C *et al*. RIP3, an energy metabolism regulator that switches TNF-induced cell death from apoptosis to necrosis. *Science* 2009; **325**: 332–336.
23. Ma Y, Temkin V, Liu H, Pope RM. NF- κ B protects macrophages from lipopolysaccharide-induced cell death: the role of caspase 8 and receptor-interacting protein. *J Biol Chem* 2005; **280**: 41827–41834.
24. He S, Liang Y, Shao F, Wang X. Toll-like receptors activate programmed necrosis in macrophages through a receptor-interacting kinase-3-mediated pathway. *Proc Natl Acad Sci USA* 2011; **108**: 20054–20059.
25. Liu B, Wang K, Gao H-M, Mandavilli B, Wang J-Y, Hong J-S. Molecular consequences of activated microglia in the brain: overactivation induces apoptosis. *J Neurochem* 2001; **77**: 182–189.
26. Koenig A, Russell JQ, Rodgers WA, Budd RC. Spatial differences in active caspase-8 defines its role in T-cell activation versus cell death. *Cell Death Differ* 2008; **15**: 1701–1711.
27. Burguillos MA, Deierborg T, Kavanagh E, Persson A, Hajji N, Garcia-Quintanilla A *et al*. Caspase signalling controls microglia activation and neurotoxicity. *Nature* 2011; **472**: 319–324.
28. Bsibsi M, Nomden A, van Noort JM, Baron W. Toll-like receptors 2 and 3 agonists differentially affect oligodendrocyte survival, differentiation, and myelin membrane formation. *J Neurosci Res* 2012; **90**: 388–398.

29. Jack CS, Arbour N, Manusow J, Montgrain V, Blain M, McCreia E *et al.* TLR signaling tailors innate immune responses in human microglia and astrocytes. *J Immunol* 2005; **175**: 4320–4330.
30. Steelman A, Li J. Poly(I:C) promotes TNF α /TNFR1-dependent oligodendrocyte death in mixed glial cultures. *J Neuroinflammation* 2011; **8**: 89.
31. Carpentier PA, Duncan DAS, Miller SD. Glial toll-like receptor signaling in central nervous system infection and autoimmunity. *Brain, Behavior, and Immunity* 2008; **22**: 140–147.
32. Cameron JS, Alexopoulou L, Sloane JA, DiBernardo AB, Ma Y, Kosaras B *et al.* Toll-like receptor 3 is a potent negative regulator of axonal growth in mammals. *J Neurosci* 2007; **27**: 13033–13041.
33. Ma Y, Li J, Chiu I, Wang Y, Sloane JA, Lu J *et al.* Toll-like receptor 8 functions as a negative regulator of neurite outgrowth and inducer of neuronal apoptosis. *J Cell Biol* 2006; **175**: 209–215.
34. Cho Y, Challa S, Moquin D, Genga R, Ray TD, Guildford M *et al.* Phosphorylation-driven assembly of the RIP1-RIP3 complex regulates programmed necrosis and virus-induced inflammation. *Cell* 2009; **137**: 1112–1123.
35. He S, Wang L, Miao L, Wang T, Du F, Zhao L *et al.* Receptor interacting protein kinase-3 determines cellular necrotic response to TNF- α . *Cell* 2009; **137**: 1100–1111.
36. Li J, Ramenaden ER, Peng J, Koito H, Volpe JJ, Rosenberg PA. Tumor necrosis factor α mediates lipopolysaccharide-induced microglial toxicity to developing oligodendrocytes when astrocytes are present. *J Neurosci* 2008; **28**: 5321–5330.
37. Kaiser WJ, Offermann MK. Apoptosis induced by the Toll-like receptor adaptor TRIF is dependent on its receptor interacting protein homotypic interaction motif. *J Immunol* 2005; **174**: 4942–4952.
38. Li J, Lin JC, Wang H, Peterson JW, Furie BC, Furie B *et al.* Novel role of vitamin K in preventing oxidative injury to developing oligodendrocytes and neurons. *J Neurosci* 2003; **23**: 5816–5826.
39. Li J, Wang H, Rosenberg PA. Vitamin K prevents oxidative cell death by inhibiting activation of 12-lipoxygenase in developing oligodendrocytes. *J Neurosci Res* 2009; **87**: 1997–2005.
40. Karlsson M, Kurz T, Brunk UT, Nilsson SE, Frennesson CI. What does the commonly used DCF test for oxidative stress really show? *Biochem J* 2010; **428**: 183–190.
41. Zhao H, Kalivendi S, Zhang H, Joseph J, Nithipatikom K, Vásquez-Vivar J *et al.* Superoxide reacts with hydroethidine but forms a fluorescent product that is distinctly different from ethidium: potential implications in intracellular fluorescence detection of superoxide. *Free Radic Biol Med* 2003; **34**: 1359–1368.
42. Duprez L, Takahashi N, Van Hauwermeiren F, Vandendriessche B, Goossens V, Vanden Berghe T *et al.* RIP kinase-dependent necrosis drives lethal systemic inflammatory response syndrome. *Immunity* 2011; **35**: 908–918.
43. Lu JV, Weist BM, van Raam BJ, Marro BS, Nguyen LV, Srinivas P *et al.* Complementary roles of Fas-associated death domain (FADD) and receptor interacting protein kinase-3 (RIPK3) in T-cell homeostasis and antiviral immunity. *Proc Natl Acad Sci USA* 2011; **108**: 15312–15317.
44. Han J, Zhong C-Q, Zhang D-W. Programmed necrosis: backup to and competitor with apoptosis in the immune system. *Nat Immunol* 2011; **12**: 1143–1149.
45. Upton JW, Kaiser WJ, Mocarski ES. Virus inhibition of RIP3-dependent necrosis. *Cell Host Microbe* 2010; **7**: 302–313.
46. Salmena L, Hakem R. Caspase-8 deficiency in T cells leads to a lethal lymphoinfiltrative immune disorder. *J Exp Med* 2005; **202**: 727–732.
47. Ch'en IL, Beisner DR, Degterev A, Lynch C, Yuan J, Hoffmann A *et al.* Antigen-mediated T cell expansion regulated by parallel pathways of death. *Proc Natl Acad Sci USA* 2008; **105**: 17463–17468.
48. Rebe C, Cathelin S, Launay S, Filomenko R, Prevotat L, L'Ollivier C *et al.* Caspase-8 prevents sustained activation of NF- κ B in monocytes undergoing macrophagic differentiation. *Blood* 2007; **109**: 1442–1450.
49. Kang T-B, Ben-Moshe T, Varfolomeev EE, Pevzner-Jung Y, Yagov N, Jurewicz A *et al.* Caspase-8 serves both apoptotic and nonapoptotic roles. *J Immunol* 2004; **173**: 2976–2984.
50. Declercq W, Vanden Berghe T, Vandenabeele P. RIP kinases at the crossroads of cell death and survival. *Cell* 2009; **138**: 229–232.
51. Festjens N, Vanden Berghe T, Vandenabeele P. Necrosis, a well-orchestrated form of cell demise: Signalling cascades, important mediators and concomitant immune response. *Biochimica et Biophysica Acta (BBA) - Bioenergetics* 2006; **1757**: 1371–1387.
52. Ginhoux F, Greter M, Leboeuf M, Nandi S, See P, Gokhan S *et al.* Fate mapping analysis reveals that adult microglia derive from primitive macrophages. *Science* 2010; **330**: 841–845.
53. Butovsky O, Siddiqui S, Gabrieli G, Lanser AJ, Dake B, Murugaiyan G *et al.* Modulating inflammatory monocytes with a unique microRNA gene signature ameliorates murine ALS. *J Clin Invest* 2012; **122**: 3063–3087.
54. Ajami B, Bennett JL, Krieger C, McNagny KM, Rossi FMV. Infiltrating monocytes trigger EAE progression, but do not contribute to the resident microglia pool. *Nat Neurosci* 2011; **14**: 1142–1149.
55. Streit WJ, Xue QS. Life and death of microglia. *J Neuroimmune Pharmacol* 2009; **4**: 371–379.
56. Fricker M, Vilalta A, Tolkovsky AM, Brown GC. Caspase inhibitors protect neurons by enabling selective necroptosis of inflamed microglia. *J Biol Chem* 2013; **288**: 9145–9152.
57. Kim S, Steelman AJ, Koito H, Li J. Astrocytes promote TNF-mediated toxicity to oligodendrocyte precursors. *J Neurochem* 2011; **116**: 53–66.
58. Mukhopadhyay P, Rajesh M, Hasko G, Hawkins BJ, Madesh M, Pacher P. Simultaneous detection of apoptosis and mitochondrial superoxide production in live cells by flow cytometry and confocal microscopy. *Nat Protocols* 2007; **2**: 2295–2301.
59. Zhao H, Joseph J, Fales HM, Sokoloski EA, Levine RL, Vasquez-Vivar J *et al.* Detection and characterization of the product of hydroethidine and intracellular superoxide by HPLC and limitations of fluorescence. *Proc Natl Acad Sci USA* 2005; **102**: 5727–5732.



Cell Death and Disease is an open-access journal published by Nature Publishing Group. This work is licensed under a Creative Commons Attribution-NonCommercial-ShareAlike 3.0 Unported License. To view a copy of this license, visit <http://creativecommons.org/licenses/by-nc-sa/3.0/>

Supplementary Information accompanies this paper on Cell Death and Disease website (<http://www.nature.com/cddis>)